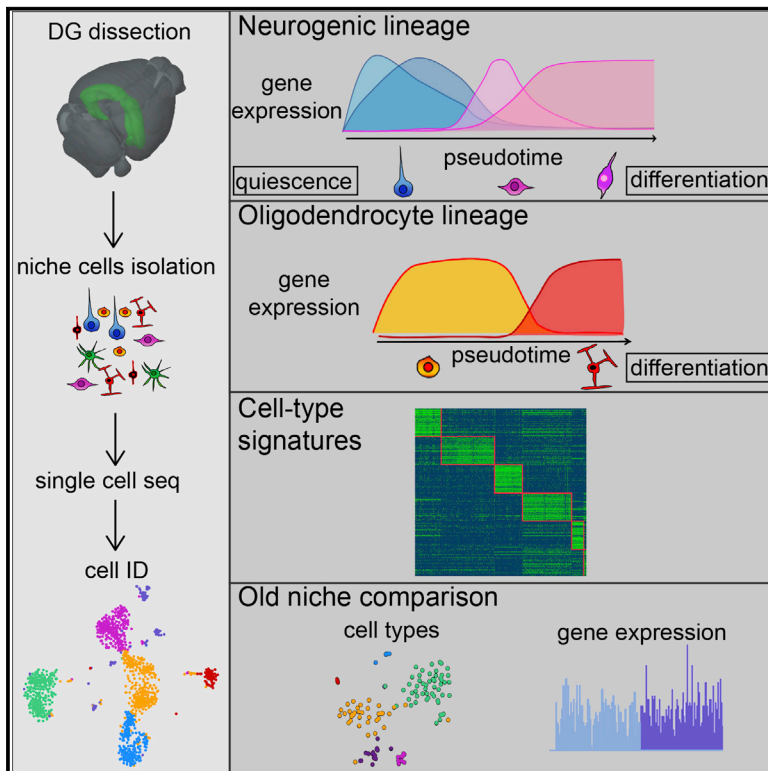


Cell Reports

A Single-Cell RNA Sequencing Study Reveals Cellular and Molecular Dynamics of the Hippocampal Neurogenic Niche

Graphical Abstract



Authors

Benedetta Artegiani, Anna Lyubimova, Mauro Muraro, Johan H. van Es, Alexander van Oudenaarden, Hans Clevers

Correspondence

h.clevers@hubrecht.eu

In Brief

Artegiani et al. perform single-cell sequencing analysis of the dentate gyrus, and they identify molecular features and lineage relations of the cell types present in the niche.

Highlights

- Single-cell sequencing identifies the cell populations in the hippocampal niche
- Dynamics of the entire neurogenic and oligodendrocyte lineages are captured
- Cell-type-specific gene signatures, including microglia activation state
- Comparison with the aged hippocampal niche

Data and Software Availability

GSE106447



A Single-Cell RNA Sequencing Study Reveals Cellular and Molecular Dynamics of the Hippocampal Neurogenic Niche

Benedetta Artegiani,¹ Anna Lyubimova,¹ Mauro Muraro,¹ Johan H. van Es,¹ Alexander van Oudenaarden,¹ and Hans Clevers^{1,2,*}

¹Hubrecht Institute, Royal Netherlands Academy of Arts and Sciences and University Medical Center Utrecht, Cancer Genomics Netherlands, Utrecht, the Netherlands

²Lead Contact

*Correspondence: h.clevers@hubrecht.eu

<https://doi.org/10.1016/j.celrep.2017.11.050>

SUMMARY

Adult neurogenesis in the murine dentate gyrus occurs in a specialized microenvironment that sustains the generation of neurons during life. To fully understand adult neurogenesis, it is essential to determine the neural stem cell (NSC) and progenitor developmental stages, their molecular determinants, and the niche cellular and molecular composition. We report on a single-cell RNA sequencing study of the hippocampal niche, performed by isolating all the non-neuronal cell populations. Our analysis provides a comprehensive description of the dentate gyrus cells, and it allows the identification of exclusive cell-type-specific markers. We define the developmental stages and transcriptional dynamics of NSCs and progenitors, and we find that, while NSCs represent a heterogeneous cellular continuum, progenitors can be grouped into distinct subtypes. We determine the oligodendrocyte lineage and transcriptional dynamics, and we describe the microglia transcriptional profile and activation state. The combined data constitute a valuable resource to understand regulatory mechanisms of adult neurogenesis.

INTRODUCTION

Neurogenesis is widespread during brain development and is essential to the formation of the CNS. In the adult brain, it is maintained in two areas: the subventricular zone (SVZ) of the lateral ventricles, where neural stem cells (NSCs) generate neurons of the olfactory bulb, and the subgranular zone (SGZ) in the dentate gyrus of the hippocampus (Kriegstein and Alvarez-Buylla, 2009; Zhao et al., 2008). In the SGZ, NSCs generate transient-amplifying progenitors that give rise to more differentiated progenitors, or neuroblasts, which ultimately produce granule neurons (Kempermann et al., 2015). Newborn granule cells integrate into the granular layer (GL), and they play critical roles in cognitive functions such as learning and memory (Gonçalves et al., 2016). The surrounding environment is essential to control these processes. In fact, the adult neurogenic areas are specialized

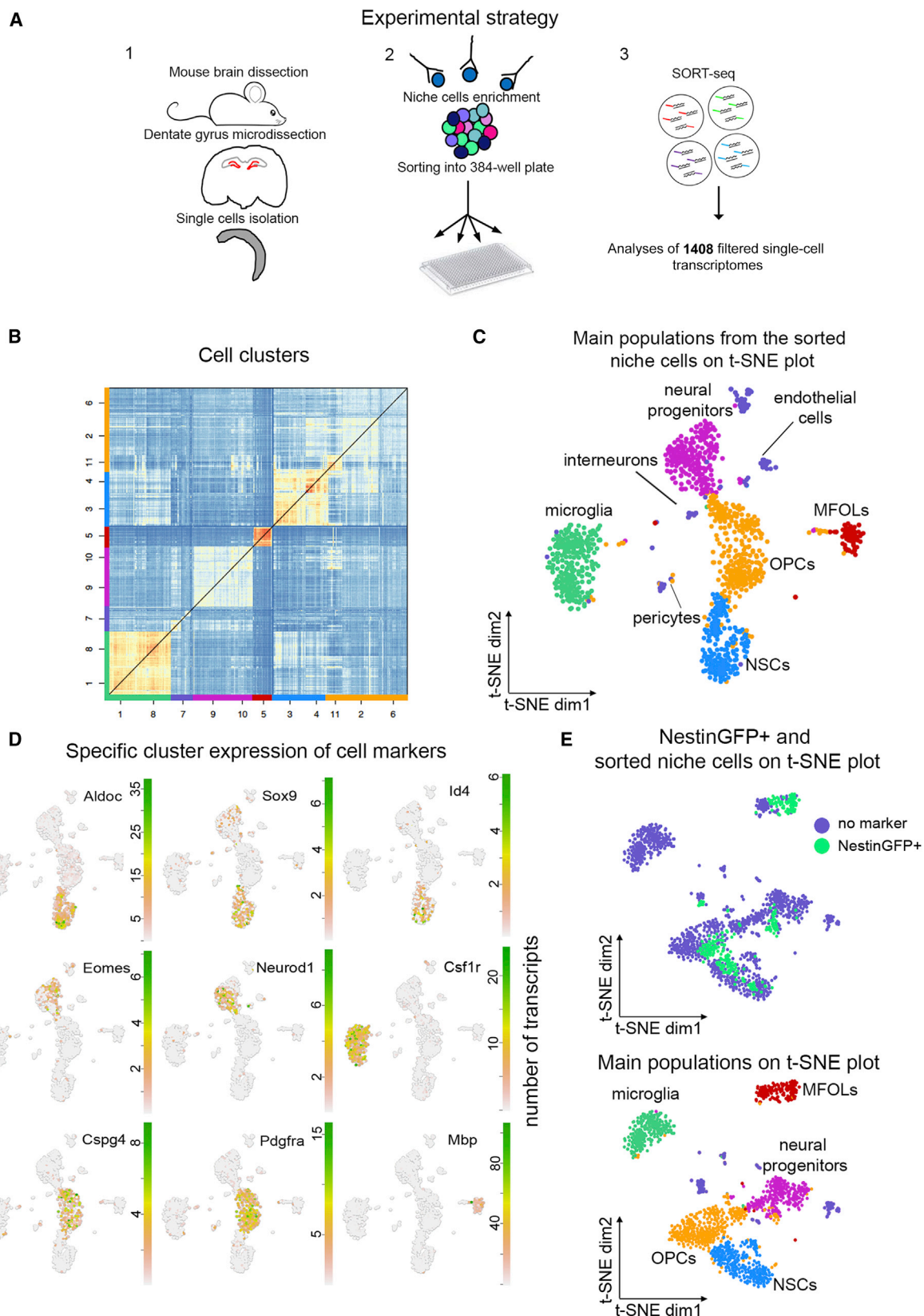
niches that provide a permissive microenvironment to allow the maintenance and differentiation of the NSCs (Ninkovic and Götz, 2013; Zhao et al., 2008). Neurogenesis is controlled by the complex interaction of the intrinsic programs of NSCs and their progressively more committed progeny, as well as exogenous signals provided to them by a plethora of niche cells (Björnsson et al., 2015).

In recent years, single-cell RNA sequencing technology has emerged as a powerful method to describe heterogeneous cell populations and measure cell-to-cell expression variability of thousands of genes (Grün and van Oudenaarden, 2015; Trapnell, 2015). In the murine and human brains, single-cell RNA sequencing studies have shed light on neural and glial cell heterogeneity (Lake et al., 2016; Marques et al., 2016; Tasic et al., 2016; Zeisel et al., 2015) and cellular and molecular dynamics during development (La Manno et al., 2016; Liu et al., 2016; Pollen et al., 2015).

The possibility to unravel the process of adult neurogenesis by single-cell sequencing has recently attracted attention. Pioneering studies on the identity of NSCs residing in the SVZ (Dulken et al., 2017; Llorens-Bobadilla et al., 2015; Luo et al., 2015) or SGZ (Shin et al., 2015) provided a better understanding of their heterogeneity. Yet, these studies focused on NSCs and not on the other constituent cells of the niche. The previously used sorting approaches allowed for the purification of only an exiguous number of the NSCs' early progeny. Therefore, a complete characterization of the neurogenic niche composition is currently lacking.

Here we aim to generate insights into the entire adult neurogenesis lineage, from NSCs to the generation of neurons. In addition, we included all other niche cells. To this end, we applied fluorescence-activated cell sorting (FACS) to label granule neurons and, by negative selection, enrich for all other cellular populations. We then performed single-cell RNA sequencing to examine the molecular features of each identified population. Our study constitutes an unbiased characterization of the cell types present in the hippocampal niche, uncovers a series of exclusive cell type markers, and provides a better understanding of the neurogenic lineage beyond the NSC dynamics. In addition, we isolated single cells from the aged dentate gyrus, and we provided a proof-of-principle demonstration that our strategy can be used to study the niche in different conditions known to affect neurogenesis.





(legend on next page)

RESULTS

Identification of Cellular Populations in the Hippocampal Neurogenic Niche

In previous single-cell transcriptomic analyses performed on adult neurogenic niches (be it the SVZ or the dentate gyrus), cells were sorted based on the expression of a known NSC marker or combinations of markers (i.e., Nestin, GFAP, Prominin1, etc.) (Dulken et al., 2017; Llorens-Bobadilla et al., 2015; Luo et al., 2015; Shin et al., 2015). We addressed the cellular heterogeneity of the entire neurogenic niche in a more unbiased fashion. Since mature granule neurons constitute the vast majority of cells in the dentate gyrus (and since these cannot be removed by dissection, given their close physical proximity to the neurogenic niche), we developed a FACS strategy to purify all non-neuronal cell types by negative selection. We microdissected and dissociated the dentate gyrus (Figure 1A). Single cells were stained with an antibody recognizing the extracellular domain of GluR1, a marker expressed in the hippocampus in mature granule cells (Hagihara et al., 2011). To avoid the preferential isolation of neuroblasts and immature neurons from the neuron-depleted population, cells were also stained with an antibody against Cd24 (Walker et al., 2013) (see the Supplemental Experimental Procedures and Figure S1A). We purified live GluR1[−]/Cd24[−] double-negative cells (Figure S1B), and we processed them for single-cell sequencing using the sorting and robot-assisted transcriptome sequencing (SORT-seq) method (Muraro et al., 2016) (Figure 1A).

A total of 3,840 single cells were sequenced. Based on a filtering criteria of 1,500 genes/cell to exclude low-quality sequenced cells, 1,109 cells were retained for analysis. Analysis was performed with the RaceID2 algorithm, which clusters similar cells by the k-medoids method (Grün et al., 2016). This clustering analysis revealed 11 populations (Figure 1B), clearly separated in the t-distributed stochastic neighbor embedding (t-SNE) map (Figure 1C). Based on the expression levels of some well-characterized marker genes (Figures 1D and S2), we defined cluster identity.

Abundant cell populations were constituted by (1) NSCs (expressing *Aldoc*, *Apoe*, *Id4*, *Hopx*, *Sox9*, *GFAP*, *Sc11a3* [GLAST], and *Sox2*); (2) neural progenitors (expressing *Eomes*, *Neurod1*, *Dcx*, and *Ccnd2*), together constituting the neurogenic lineage; (3) oligodendrocyte progenitor cells (OPCs; expressing *Olig1*, *Olig2*, *Sox10*, *Pdgfra*, and *Cspg4*, also known as *Ng2*); (4) myelin-forming mature oligodendrocytes (MFOLs; expressing *Plp1*, *Mal*, *Mog*, and *Mbp*), belonging to the oligodendrocyte lineage; and (5) microglia cells (expressing *Csf1r* and *Cx3cr1*). Astrocytes were also found. However, these did not cluster separately from the NSCs, underlining the close similarity

between these two cell types and the glial nature of NSCs. Many of the NSC markers are shared with astrocytes, but the latter population expresses high levels of specific astrocytic markers, such as *S100β* and *Fzd2*. Only a few *S100β*⁺ cells were found within the NSC cluster (Figure S2).

To validate our approach and to exclude that our defined NSC cluster mostly consisted of astrocytes, we sequenced 384 GFP⁺ cells isolated from the hippocampus of *Nestin*^{GFP} mice (Mignone et al., 2004) (Figure S3A), previously used as an NSC marker (Shin et al., 2015), and we compared them to the cells present in our dataset. 299 *Nestin*⁺ cells were retained after filtering out low-quality cells. The clustering revealed 4 main clusters on the t-SNE plot (Figure S3B) that, based on specific marker expression (Figure S3C), were identified as NSCs, a small number of neural progenitors that retained Nestin expression, and both OPCs and MFOLs. This is in agreement with previous reports showing that the use of Nestin or other NSC marker leads to the isolation of cells with an oligodendrocyte signature (Shin et al., 2015; Dulken et al., 2017). We combined the datasets obtained from *Nestin*^{GFP}⁺ cells with cells sorted based on no marker expression, and we clustered the 1,408 high-quality cells. They clustered together on the t-SNE plot (Figure 1E, top) and according to their cellular type (Figure 1E, bottom). Altogether, these data corroborate the cell identification in our dataset. We also showed that, while all the cell types that can be identified based on Nestin expression can be found as well in our dataset, *Nestin*⁺ cells represent only a subset of cells that are isolated by our negative sorting approach.

We found other smaller populations that we identified as interneurons (expressing *Reln* and *Ndnf*), pericytes (expressing *Tbx18*, *Vtn*, and *Col1a1*), and endothelial cells (expressing *Vwf*) (Figure S2), which clustered together (Figure 1B). An additional cell cluster did not express any of the known markers of the previously defined cell populations, yet it expressed high levels of *Ptpcr* (better known as Cd45). Cd45 is a marker for all hematopoietic cells, whose expression is downregulated in microglia cells. These rare Cd45^{high} cells were clearly distinct from the Cd45^{low} microglia cells (Figure S2). Based on current knowledge about immune cells in the CNS (Prinz and Priller, 2014), the Cd45^{high} cluster could represent infiltrating or vasculature macrophages.

Analysis of the Neuronal Lineage Reveals Molecular Hallmarks along the Trajectories of NSC Activation and Progenitor Differentiation

We decided to analyze the neurogenic and oligodendrocyte lineages in detail to define cellular developmental stages and gene expression changes along the differentiation trajectories. We first focused on cells defined by the first level of clustering

Figure 1. Identification of Cell Populations in the Dentate Gyrus Neurogenic Niche

- (A) Scheme of the experimental approach. (1) The dentate gyri were isolated and microdissected, and single cells were isolated and (2) depleted of the neurons by staining with the GluR1 and Cd24 antibodies. Single double-negative cells were sorted into 384-well plates and (3) processed.
- (B) Heatmap representing transcriptome similarities between cells. Numbers on the axis represent the clusters identified in the first clustering level, and colors show clusters grouped together as belonging to the same cell population.
- (C) t-SNE map of the clusters obtained with the RaceID2. Colors represent cell population clusters as in (B).
- (D) t-SNE maps showing the expression of representative markers for each population. Transcript counts are in linear scale.
- (E) t-SNE maps representing the clustering obtained by the combined dataset of 1,408 cells derived by *Nestin*^{GFP}⁺ and negatively sorted cells. The t-SNE map on top shows the origin of the analyzed cells (*Nestin*^{GFP}⁺, green; negatively sorted cells, violet), and the bottom one shows cluster identity, with colors as in (C).

as belonging to the neurogenic lineage. We selected these cells (424 cells) and performed a second round of clustering. The cells separated into 2 main clusters in the t-SNE plot (Figure 2A), NSCs and neural progenitors, which agrees with the first level of clustering results (see Figure 1C). Subclustering revealed multiple subpopulations, suggesting that NSCs and progenitors do not represent homogeneous populations but rather different developmental stages. To determine the differentiation trajectory and gene expression signatures along this trajectory, we ordered the single cells on the pseudo-temporal axis and investigated gene expression dynamics by using StemID (Grün et al., 2016). StemID performs temporal ordering based on the concept that less differentiated cell types have higher transcriptomic entropy (Grün et al., 2016). We were then able to group genes based on their expression along this temporal axis (Figure S3C).

By inspecting temporal patterns of gene expression, we found that some genes commonly used as NSC markers were not evenly expressed in the NSC subpopulation (Figure 2B). Furthermore, temporal gene expression patterns did not allow us to clearly separate discrete subpopulations. Our results are consistent with a model where NSCs represent a continuum of intermediate developmental stages, in which quiescent stem cells progressively proceed toward generation of the actively proliferating neural progenitors. This developmental progression is characterized by differential expression of specific NSC genes (Figure 2B). Expression of hallmark genes of quiescence (such as, for instance, *Apoe*, *Clu*, *Aldoc*, and *Id3*) was high in the earliest developmental stages and decreased at later stages. Genes that have been linked with NSC activation, such as *Fgfr3* (Kang and Hébert, 2015), tend to increase their expression along the pseudo-temporal axis. Some NSC markers instead, such as *Sox9*, were evenly expressed along NSC developmental stages (Figure 2B). More mature NSCs started to express low levels of genes characteristic of the neural progenitor state (e.g., *Sox11* and *Hmgn2*). In agreement with previous reports (Shin et al., 2015), proliferation markers were lowly expressed in the NSCs, and they were detected when cells entered the S-phase and started expressing progenitor markers (Figure 2B).

Our analysis showed that neural progenitors are clearly distinct from NSCs. With few exceptions, NSC-specific genes are not expressed in neural progenitors and vice versa. In contrast to NSCs, neural progenitors can be categorized into more discrete subpopulations expressing different genes, e.g., *Eomes*, *Ccnd2*, and *Hmgn2* for the earlier population and *Neurod1*, *Sox11*, and *Dcx* for the late progenitors (Figures 2B, S4A, and S4D). An intermediate state between the early and late progenitors could also be recognized (Figures 2B and S4D). Compared to the more terminally differentiated late progenitors, the early progenitors expressed higher levels of proliferation genes (e.g., *Ccnd2*, *Mki67*, *Pcna*, *Mcm2*, and ribosomal subunits genes) (Figure S4D; data not shown).

A previous single-cell sequencing study of the SGZ NSCs revealed the temporal gene regulation occurring during NSC differentiation (Shin et al., 2015). However, the number of isolated progenitors in that study was exiguous (Figure S4B). Progenitors did not form a cluster distinct from NSCs, and it was not possible to distinguish progenitor subtypes (Figure S4B). In contrast, we were able to determine both progenitor subtype identity and

cascade of gene expression during progenitor differentiation with high resolution (Figures S4A, S4C, and S4D).

To compare the cells belonging to the neurogenic lineage (isolated by negative FACS) with the Nestin⁺ neurogenic cells, we combined the two datasets and we ordered cells together on pseudo-time (Figure S5). As previously shown by clustering, Nestin⁺ NSCs did not differ from our negatively sorted NSCs. They were similarly distributed on the pseudo-time axis, and within both populations we could retrieve cells belonging to all stages and expressing similar levels of developmentally regulated genes (Figure S5). Instead, the Nestin⁺ progenitors provided an under-representation of the total neural progenitor developmental stages that we could isolate with our sorting.

To validate our results by a second, independent method, we used the Waterfall pipeline (Shin et al., 2015). Waterfall differs from the RaceID2 by several aspects. First, cells are clustered based on unsupervised hierarchical clustering. Second, the cells are aligned on pseudo-time by similarity between single-cell transcriptomes, after defining the order of the lineage trajectory based on the expression of known markers, as visualized in principal-component analysis (PCA) plots. The results obtained with the Waterfall pipeline confirmed our previous conclusions. Unsupervised hierarchical clustering and PCA analyses (Figure 2C, left and middle) showed that NSCs and progenitors are distinct and that, while the NSCs constitute a continuum of cells, the progenitors can instead be grouped into more discrete cell populations. The temporal gene expression patterns within the two independent analyses showed a good similarity (Figure 2C, right, and Figure 2B).

Our data analysis unraveled gene expression cascades of NSC and progenitor subtypes.

Identification of Oligodendrocyte Subtypes Present in the Neurogenic Niche and Their Lineage Relation

The second major group of cells that we identified in our dataset was constituted by oligodendrocytes. Those cells were always excluded from previous single-cell sequencing analyses of the SVZ and SGZ (Dulken et al., 2017; Llorens-Bobadilla et al., 2015; Shin et al., 2015). As opposite to the rare NSCs, oligodendrocytes in the adult brain are widespread, but they display a high degree of regional heterogeneity (Marques et al., 2016). Therefore, in order to characterize the oligodendrocyte precursors and mature cells that are present in the hippocampal niche, we selected the pertinent cells (333 cells) and performed a sub-clustering analysis. In addition to the OPCs and MFOLs revealed by our first clustering level, we detected a small number of committed oligodendrocyte precursors (COPs) (Figure 3A). This population was characterized by the following specific markers: *Bmp4*, *Fyn*, and *Gpr17*. Analysis by RaceID2 clustered the OPCs into 3 subclusters, while the MFOLs appeared as a single homogeneous cluster (Figure 3A).

After ordering the cells along the pseudo-time and analyzing the gene expression patterns along this developmental trajectory, we found that the OPCs are a much less heterogeneous population as compared to, for instance, the neural progenitors. Minor differences concerned the expression level of genes, such as *Olig1*, *Olig2*, and *Pdgfra*, which showed a less pronounced expression in the earlier developmental stages (Figure 3B), and

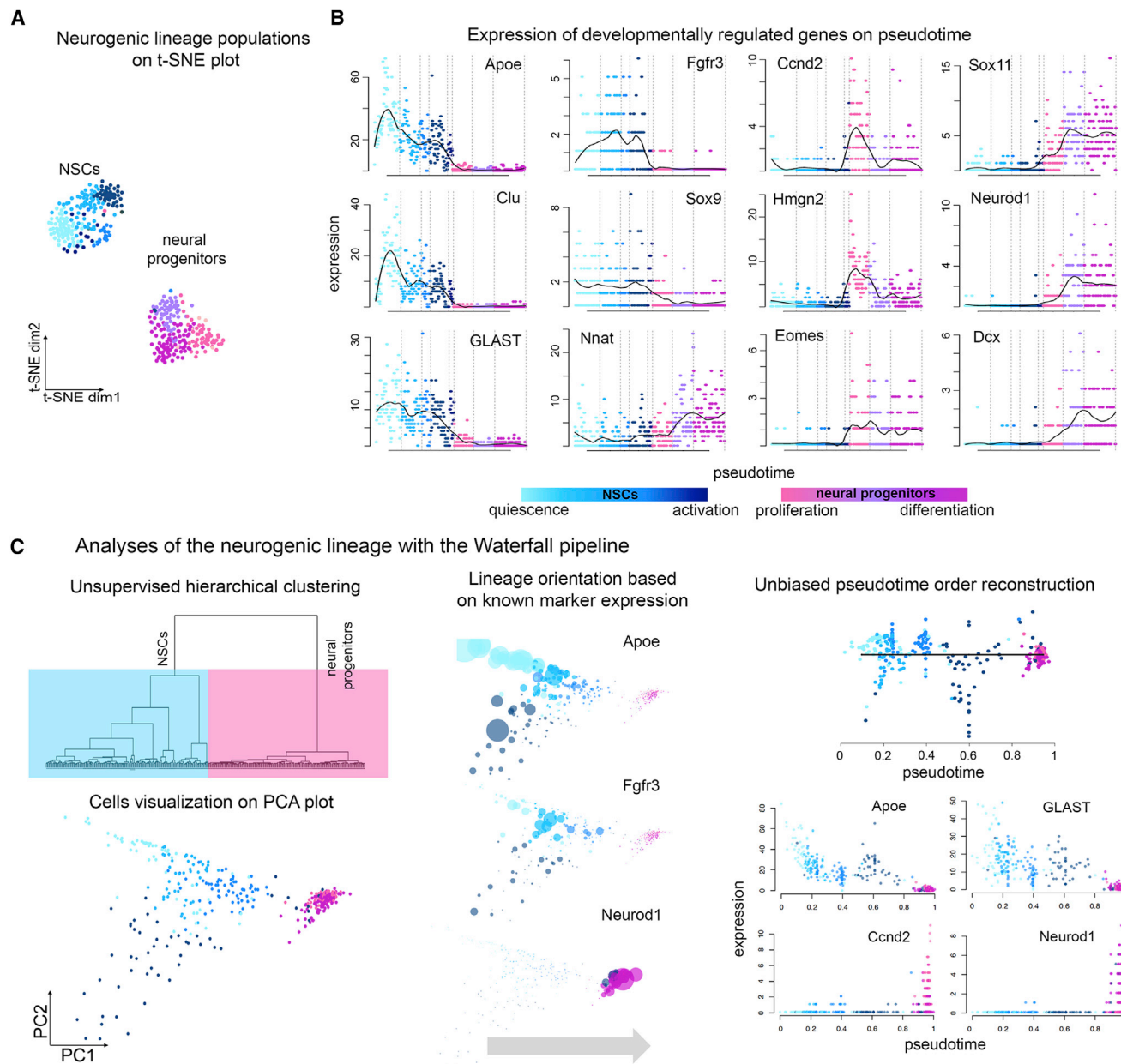


Figure 2. Analysis of the Neurogenic Lineage

(A) t-SNE map representing the subclustering analysis of cells belonging to the neurogenic lineage. Colors (blue and pink) refer to NSCs and neural progenitors as identified in the first-level clustering, and gradients identify subclusters determined in the second-level clustering.

(B) Expression profile of representative genes along the pseudo-time. Gene expression is shown on the y axis as transcript counts (the black line is the running mean of expression with a window size of 25 cells). Each dot represents a cell and cells are highlighted in the same subcluster color gradient as in (A). Cells were ordered on the x pseudo-time axis by StemID. Genes are ordered based on expression gradient with respect to the pseudo-time, and they were chosen as representative examples of pseudo-timed differential expression along the transition from quiescence to activation for NSCs and proliferation to differentiation for neural progenitors.

(C) Analysis of the neurogenic lineage using the Waterfall pipeline. Unsupervised clustering of the cells belonging to the neurogenic lineage (left, top) is shown. The same color code as in (A) is maintained. PCA plot (left, bottom) and expression of known representative markers in the clusters (middle) allowed determining the orientation of the differentiation trajectory (gray arrow). Each dot is a cell and the sizes of the dots represent the relative expression levels of the indicated transcript. Pseudo-time ordering (right, top) is obtained by defining the relative position of each cell on the differentiation trajectory based on transcriptomic differences and spanning tree reconstruction. Representative expression profiles of pseudo-timed-regulated genes (right, bottom) are shown. Cells are colored in the same color gradient representing subclusters in the PCA plot.

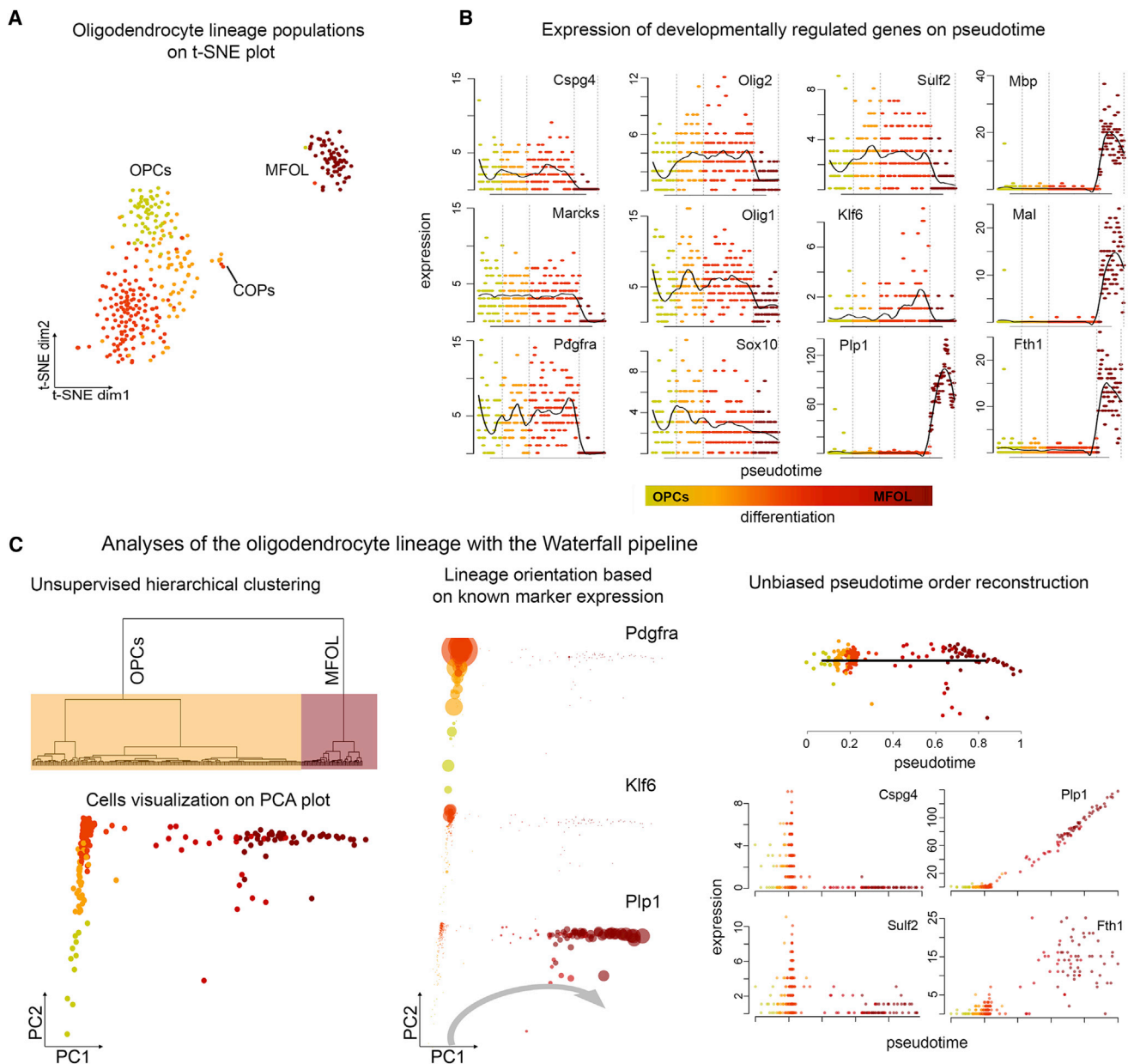


Figure 3. Analysis of the Oligodendrocyte Lineage

(A) t-SNE map representing the subclustering analysis of the cells belonging to the oligodendrocyte lineage. Colors (orange and dark red) refer to OPCs and MFOLs as identified in the first-level clustering, and gradients identify subclusters determined in the second-level clustering.

(B) Expression profile of representative genes along the pseudo-time. Gene expression as transcript count is on the y axis and the running mean is in black. Each dot represents a cell and cells are highlighted in the same color gradient representing subclusters in (A). OPCs and MFOLs belonging to different subclusters were ordered on the x pseudo-time axis by StemID.

(C) Analyses using the Waterfall pipeline. Unsupervised clustering of the cells belonging to the oligodendrocyte lineage (left, top) is shown. The same color code as in (A) is maintained. PCA plot (left, bottom) and expression of known markers in the clusters (middle) allowed determining the orientation of the differentiation trajectory (gray arrow). Each dot is a cell and its size represents the expression level of the indicated transcript. Representative expression profiles of pseudo-timed-regulated genes (right, bottom) are shown. Cells are colored in the same color gradient representing subclusters in the PCA plot.

of some differentiation genes, such as *Klf6*, which displayed higher expression in the later stages (Figure 3B). In the transition from OPCs to MFOLs, most of the genes displayed an on/off expression pattern, except for rare genes such as *Olig1* and *Olig2* that were detected in all populations, albeit at different

levels (Figure 3B). Interestingly, the analysis of temporal gene expression allowed us to identify marker genes that have not been previously seen in specific oligodendrocyte stages, such as *Marcks*, *Sulf2*, and *Fth1*. Our results were validated by analysis using the Waterfall pipeline (Figure 3C).

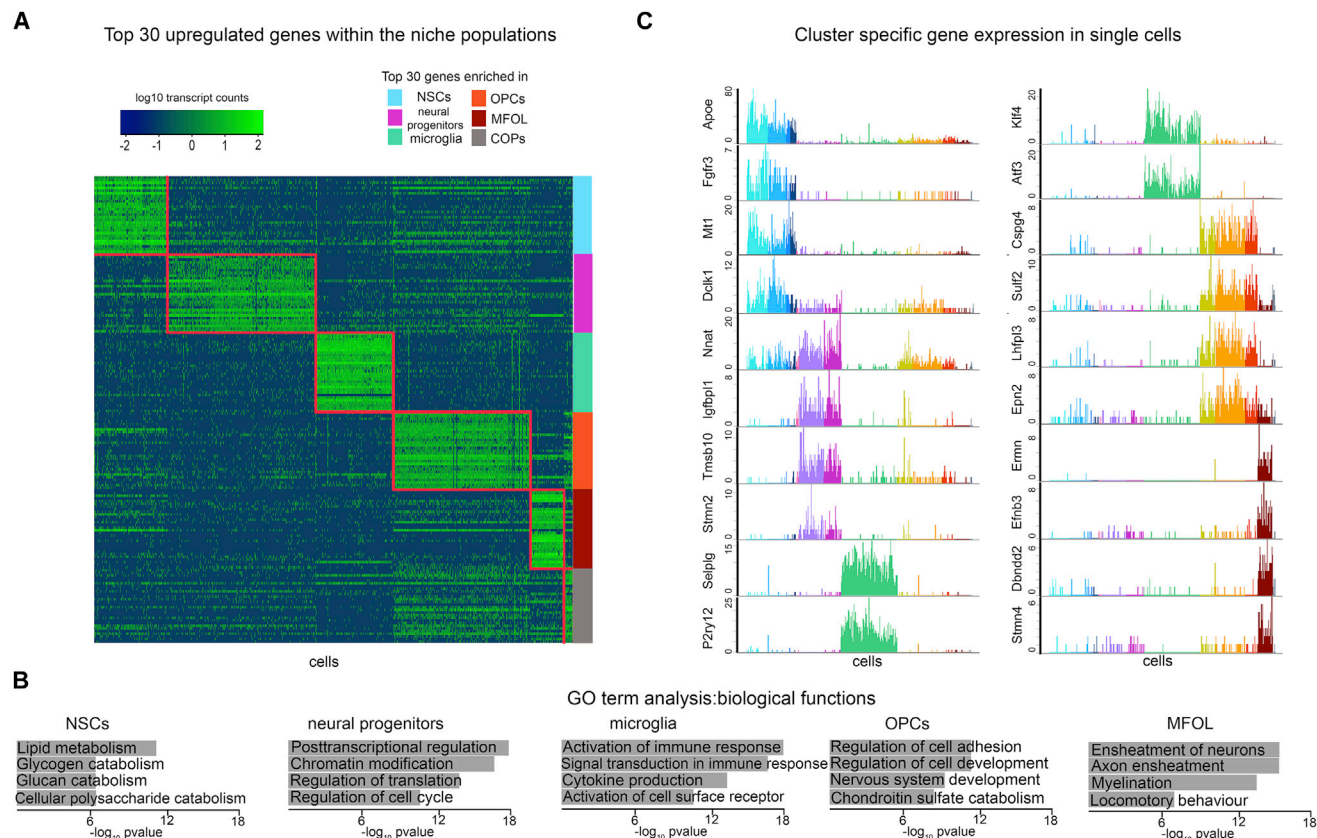


Figure 4. Identification of Cell-Specific Gene Signatures

(A) Heatmap of the expression of the top 30 upregulated genes in each of the main cell clusters. Each column represents a cell and each row represents a gene. Genes are grouped based on specific cluster expression and cells are ordered based on clustering.

(B) GO term analyses for the cluster-specific gene biological functions. The top five GO terms on a rank-based ranking were selected for each cell-type-specific gene signature.

(C) Barplots showing the expression of representative cluster-specific genes within the total 1,109 cell data frame. Each bar represents a cell and cells are grouped based on clustering, with the same color code as for the original clusters.

Our data determined the oligodendrocyte stages present in the hippocampal niche, and they unraveled their gene expression cascade.

Identification of Cluster-Gene Expression Signatures and New Cell-Type-Specific Genes

The fact that our dataset is not restricted to NSCs gave us the possibility to first investigate the gene expression signatures that are specific for a certain cell type; to identify unknown cell-type-specific genes; and to finally link the gene signature of a given cell type with its biological functions, to give hints about the role of genes with restricted expression patterns.

We repeated the clustering but using more stringent filtering criteria. We retained cells in which 4,000 genes were sequenced and each was detected at least in 2 cells, with a minimum threshold of 4 mRNA molecules/cell. Even with these filters, 654 cells could be retained for analysis. The clustering was not affected, and the same cell populations identified Figure 1C were detected (Figure S6B). We compared each main cluster to the others to identify differentially expressed genes within the considered population (p value $< 10^{-3}$). We found that

591 genes were uniquely upregulated in NSCs as compared to other populations analyzed in this study, 1,065 in neural progenitors, 681 in microglia, 703 in OPCs, 81 in COPs, and 407 in MFOLs (see Table S1 for the gene lists and Table S2 for the mean and variation of gene expression). Some additional rare cell types were also present, albeit in very low proportions, and for some of them (pericytes, interneurons, and Cd45^{high} population) we also identified cluster-specific genes (Table S1). Plot of the expression of the top 30 genes from each main cell-type-specific gene list showed that the identified signatures are highly specific (Figure 4A).

To obtain insights into the biological functions of these genes, we performed gene ontology (GO) term analysis by using the entire set of significantly upregulated genes in each population. This showed that the cluster-specific gene signatures reflect the biological function of the corresponding cell type. Many genes enriched in NSCs were related to glucose (e.g., *Gadph*, *Aldoc*, *Aldoa*, and *Pgk*) and lipid metabolism (e.g., *Fasn*, *Fabp5*, *Fabp7*, *Acsl3*, *Acsl6*, *Apoe*, *Gpld1*, and *Fasn*) (Figure 4B), in agreement with previous *in vivo* reports (Knobloch et al., 2013). Genes expressed in neural progenitors instead were associated

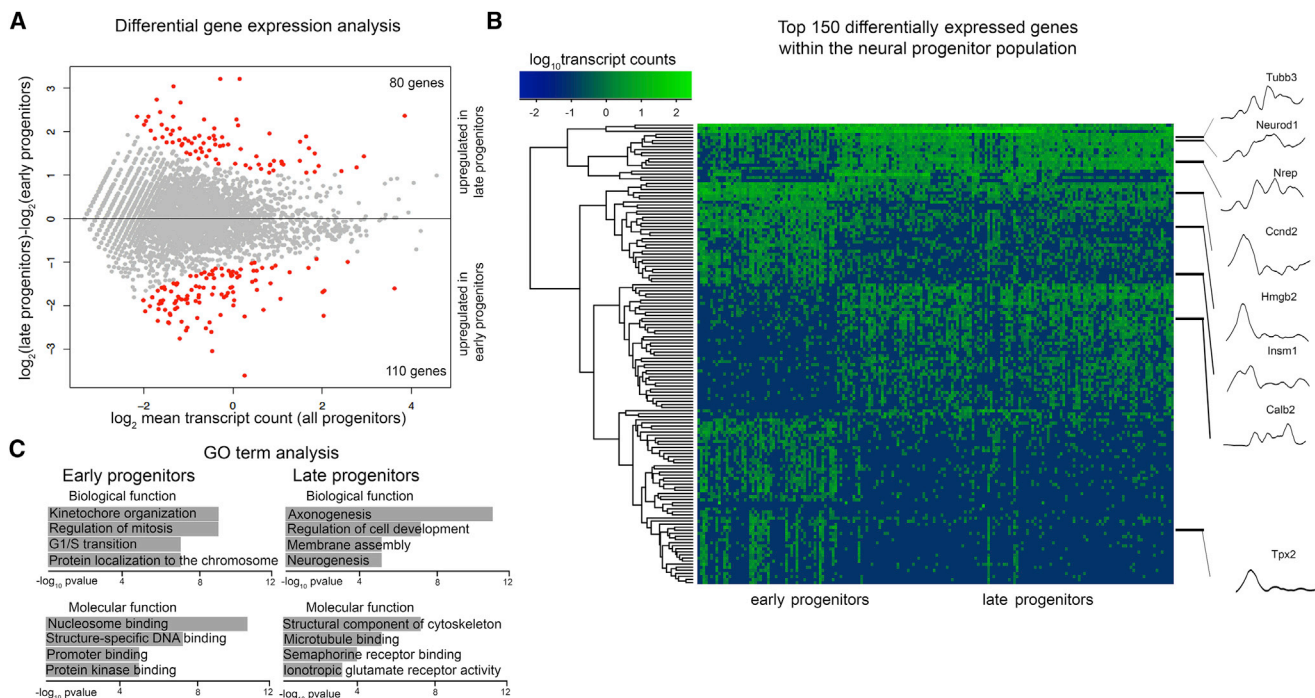


Figure 5. Gene Expression Signature of Progenitor Subtypes

(A) Dot plot of the differential gene expression analysis between progenitor stages. Gray and red dots are genes not significantly or significantly changed (p value $< 10^{-3}$), respectively. The \log_2 mean of the transcript count is on the x axis and the \log_2 fold change is on the y axis.

(B) Heatmap of the expression of the top 150 differentially regulated genes. Each column represents a cell and each row represents a gene. Genes are ordered based on unsupervised clustering and cells on subclustering. Expression for some of the representative genes along the pseudo-time is shown (right).

(C) Top five GO terms for the differentially expressed genes.

with gene expression control and cell cycle progression. The microglia-specific genes were mostly involved in the immune response. Genes upregulated in the oligodendrocyte subtypes were related to oligodendrocyte development, cell migration, and adhesion for OPCs and COPs, and myelination and axon ensheathment for the MFOLs (Figure 4B).

To further validate the robustness of our differential gene expression analysis and the cluster-specific expression, we plotted the expression of selected genes in each of the 1,109 cells in our dataset. Among the top differentially expressed genes, we plotted the expression of known marker genes, as well as the markers that have been identified by our analyses (i.e., *Mt1*, *Dcl1*, *Nnat*, *Igf1*, *Tmsb10*, *Stmn2*, *Sulf2*, *Lhfp13*, *Ernm*, *Epn2*, *Ernm*, *Efnb3*, *Dbn2*, and *Stmn4*). All genes displayed a restricted expression and can be considered as exquisite markers (Figure 4C).

Finally, we selected the top 5 genes for every population, and we inspected their expression in the *in situ* Allen brain atlas. Cell location, distribution, number, and morphology of the positive cells (Figure S6A) suggested expression of the marker genes in the proper cell type (Figure S6C), although co-immunostaining with known markers would be required in the future for a final validation for each individual marker.

Thus, our data provide the specific gene signature and a range of putative markers for the various cell types of the hippocampal niche.

Gene Expression Analysis Reveals Molecular Cascades Involved in Neural Progenitor Differentiation

We have shown that our dataset constitutes a valuable resource to investigate cell-type-specific gene signatures. We have also shown that, in contrast to other populations, such as the NSCs (a continuum of heterogeneous cells) and the OPCs (a rather homogeneous population), the neural progenitors can be subdivided into distinct and discrete subpopulations (Figures 2 and S4). Therefore, we performed differential gene expression analyses among progenitor subtypes. First, we selected the 1,065 genes enriched in the neural progenitor cluster, and we compared their expression among each subtype (early, intermediate, and late progenitors, as in Figures 2A and 2B). Only a small number of genes (13) were differentially expressed in the intermediate state. Comparison of these 3 populations suggested that the intermediate stage represents a more committed cell state that retains expression of genes typical of the early progenitors (see Figure S4D). We therefore grouped intermediate and late progenitors together as late progenitors. 80 genes were upregulated in the late progenitors and 110 in the early progenitors (p value $< 10^{-3}$) (Figure 5A). Unsupervised hierarchical clustering of the top 150 differentially expressed genes revealed distinct gene signatures for the two progenitor subtypes (Figure 5B), which matched with their expression pattern along the pseudo-time (Figure 5B, right).

To investigate the biological significance of these signatures, we performed GO term analyses. The genes characteristic of the early progenitors were related to cell cycle regulation and transcriptional activation. Instead, the late progenitor-expressed genes were relevant for the generation of newborn neurons and for molecular functions predominantly connected with cytoskeleton organization and neurotransmitter receptor activity (Figure 5C).

We found a high number of transcription factors among the genes specifically enriched in progenitors (Table S3). This probably underscores the importance of transcriptional cascades in the switch from NSCs to progenitors and neural progenitor development. We focused on transcription factors that were enriched in progenitors and on those that were differentially expressed between the two main progenitor populations (Table S3). Among these, there were known regulators of pattern specification (e.g., *Emx1*, *Emx2*, *Dlx2*, *Bmi1*, *Foxg1*, and *Eomes*) (Brill et al., 2008; Hodge et al., 2013; Yoshida et al., 1997) and neuronal differentiation (*Sox11*, *Neurog2*, *Neurod1*, and *Neurod2*) (Ninkovic et al., 2013) and chromatin remodelers (e.g., *Hdac2*, *Smarca4*, and *Smarca2*), but also many transcription factors whose function has not been described in the context of adult hippocampal neural development (e.g., *Hmgn2*, *Lhx2*, *COUP-TF1/Nr2f1*, *Pbx1*, *Cbx3*, *Maged1*, and *Ssbp3*). Thus, our data constitute a valuable resource for future studies on molecular mechanisms regulating neurogenesis.

Identification of Dentate Gyrus Microglia Signature

Our data revealed that microglia cells constitute a prominent cell population within the hippocampal niche. Microglia are the parenchymal macrophages of the CNS (Gomez Perdiguero et al., 2013). They have been implicated in critical functions in the hippocampal niche, such as the clearance of the debris derived from the massive apoptotic process of newly generated neurons, both in homeostatic and disease conditions (Abiega et al., 2016; Sierra et al., 2010). We analyzed the molecular signature of microglia at the single-cell level. First, we investigated dynamics of gene expression in the microglia cluster. We selected genes that were microglia specific (Table S1), and we analyzed their expression within the cluster. This revealed a substantial homogeneous expression of most of the highly enriched genes. Some markers commonly used to identify microglia, such as *Aif1* (also known as *Iba1*), were not expressed in all cells (Figure 6A). Instead, dentate gyrus microglia expressed high levels of *Csf1r* (which is a main regulator of the microglia lineage; Gautier et al., 2012), *Cx3cr1*, and *Tyrobp* (Dap12) (Figure 6A). Besides these classical microglia markers, we found many other genes to be specifically and highly expressed, such as *P2ry12*, *Hexb*, *Gpr34*, *Ctss*, *Cts3*, *Siglech*, *Fcrls*, *Selp1g*, *Tmem119*, *Olfml3*, *Fcgr3*, *Rgs2*, *Laptm5*, and *Trem2* (Figure 6A). Some of these seem to be specific for microglia, as their expression was not detected in RNA sequencing of macrophages both from the spleen and peritoneum (Butovsky et al., 2014; Hickman et al., 2013). As mentioned, we could detect a small number of *Cd45^{high+}* cells that clustered apart from the *Cd45^{low+}* microglia. While co-markers for the two populations were identified (e.g., *Selp1g* and *Laptm5*), several of the microglia-specific genes were almost undetectable in the *Cd45^{high+}* cluster (Figure 6B).

We then inspected our data to look at the dynamics of microglia activation. Microglia in the brain can be activated to be primed in two ways: the canonical M1 priming state promotes inflammation and the consequent neurotoxicity, and the alternative M2 priming state has an anti-inflammatory function aimed at restoring homeostasis and promoting regeneration (Cherry et al., 2014; Prinz and Priller, 2014; Sasaki, 2017). Some genes that can be considered as markers of the two states have been characterized (Chhor et al., 2013; Colton, 2009). Generally, we found that the expression of these activation genes was very low in the hippocampal microglia. However, the expression of some of the alternative markers (*Ccl2*, *Gas6*, and *Tgfb1*) was detectable (Figure 6C, bottom) and higher than most of the canonical markers (Figure 6C, top). *Trem2*, suggested to be expressed in M2 activation (Neumann and Takahashi, 2007), was also identified as one of the cluster-specific genes in the dentate gyrus microglia (Figure 6A). Our data provide evidence that the dentate gyrus microglia is in a neuroprotective state, in agreement with its important role in removing cell debris to ensure homeostasis of the niche (Sierra et al., 2010).

The Effect of Aging on the Hippocampal Neurogenic Niche

Adult neurogenesis is affected by several disease conditions, as well as by aging (Gonçalves et al., 2016). Although it is clear that neurogenesis is decreased during aging, the specific effects on the different cell types are not entirely understood (Artegiani and Calegari, 2012). To investigate possible consequences induced by aging in the hippocampal niche, we isolated the neuronal depleted-cell populations from the dentate gyrus of >1-year-old mice. In total, we sequenced 384 cells, resulting in 130 high-quality single-cell transcriptomes. We performed clustering (Figure 7A), and, based on specific cell marker expression in the different clusters (Figure 7B), we defined cell identity in the t-SNE plot. We identified all main cell populations that we had isolated previously from the young niche. Relative numbers of these cells were different in the old niche (Figures 7A and 7B). In fact, the most abundant population was constituted by immune cells, in first instance microglia but also *Cd45^{high}* cells. OPCs were also present in high numbers, while MFOLs constituted a relatively small group. However, the most striking difference was constituted by the fact that a very small number of NSCs could be identified (4.7% of total analyzed cells) with a lower NSC/neural progenitor ratio. Neural progenitors were also less abundant than in the young niche, and they expressed mostly markers of later maturation stages (e.g., *Neurod1* and *Sox11*; Figure 7B). Of note, in the independent sorting and sequencing experiments we performed on young mice, cell populations were within a similar range (e.g., NSCs represented 23% ± 5% of the total). Therefore, the observed changes in cell type ratios appear to reflect a real biological effect, and they are unlikely to be due to dataset size difference.

Next, we investigated whether the different cell types isolated from the old niche displayed molecular differences as compared to their young counterparts. We combined datasets from old and young mice, and we visualized the clustering analysis results of the total 1,239 high-quality single transcriptomes in a t-SNE plot (Figure 7C). Aged and young cells clustered together

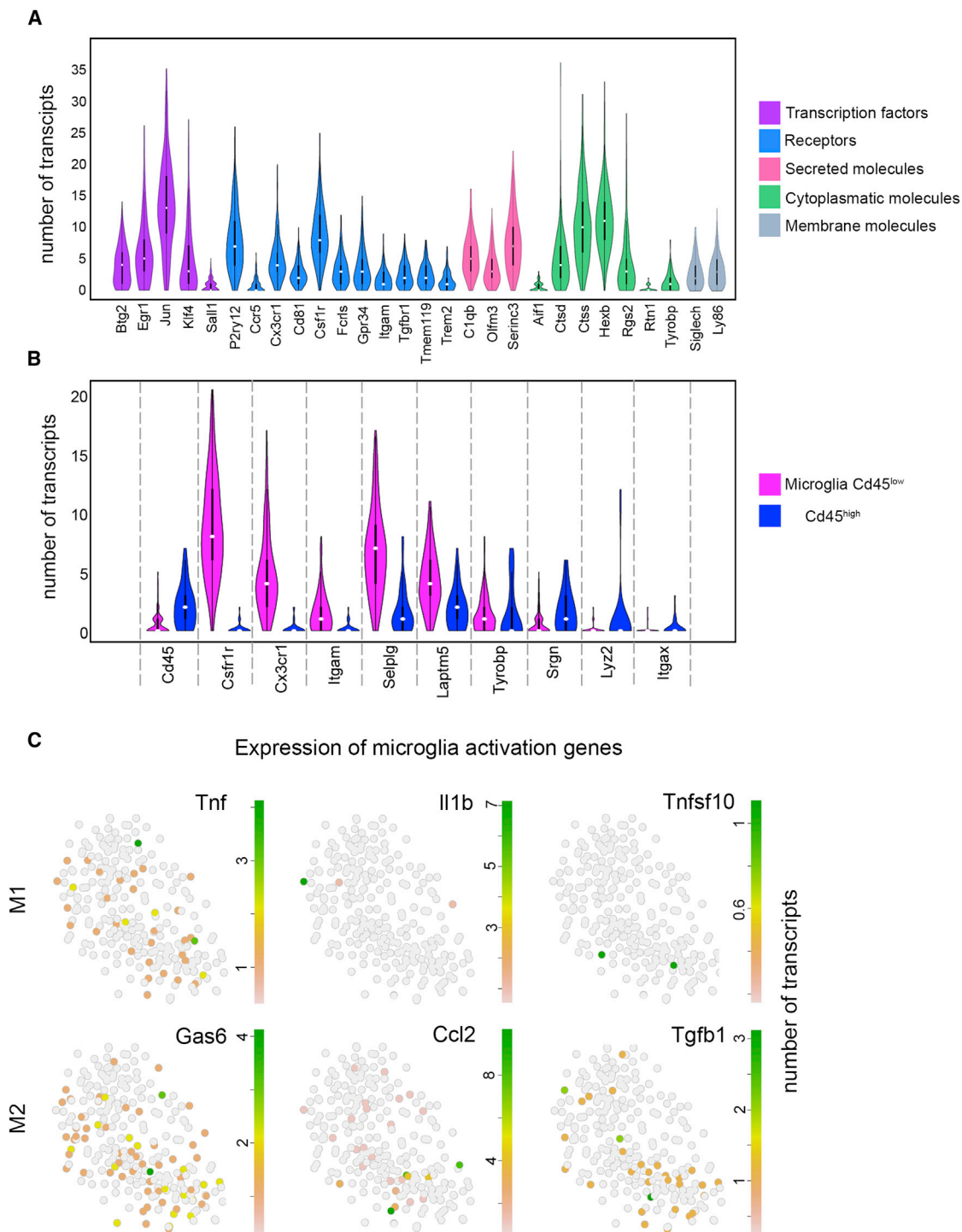


Figure 6. Dentate Gyrus Microglia Signature

(A) Violin plots showing the expression of genes enriched in microglia. Genes are grouped based on localization/function.

(B) Violin plots comparing expression level between Cd45^{high} cells and Cd45^{low} microglia for microglia- and macrophage-specific genes.

(C) t-SNE maps showing the expression of representative marker genes for the M1 (top) and M2 (bottom) activation states. Transcript counts are in linear scale.

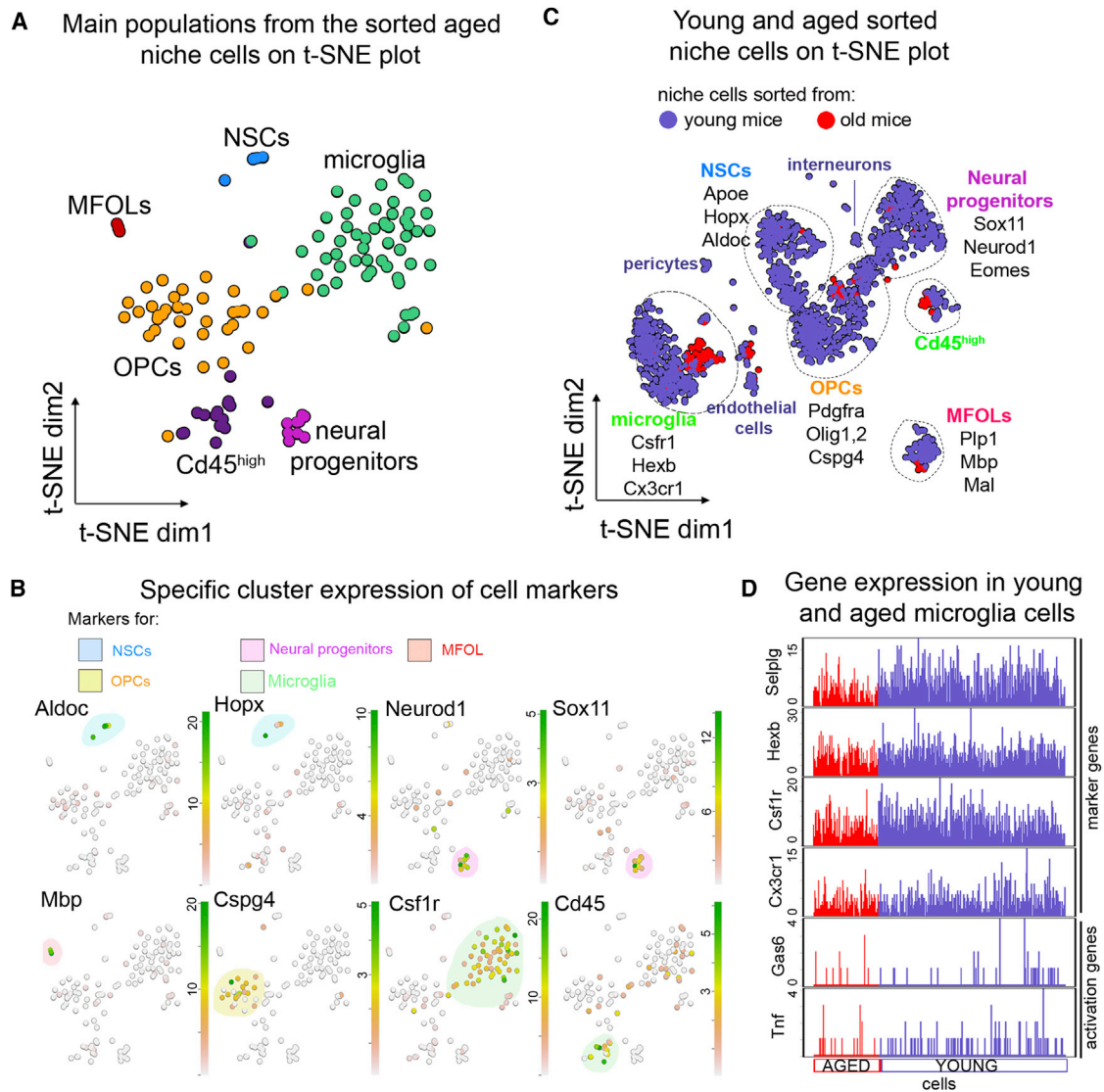


Figure 7. Analysis of Cell Populations in the Aged Hippocampal Niche

(A) t-SNE map of the clusters obtained from cells isolated from the dentate gyrus of mice >1 year old. Colors represent cell population clusters as in Figure 1A. (B) t-SNE maps showing the expression of representative marker genes for each cell population. Transcript counts are in linear scale. (C) t-SNE map of the clusters obtained by the combination of single-cell transcriptomes from young (violet) and aged (red) niche. (D) Barplots showing the expression of representative microglia markers and activation genes within the microglia isolated from young (violet) and aged (red) mice.

according to their cell type (Figure 7C), suggesting that molecular differences between cells from the young and aged niche are not major. Interestingly, functional changes in the dentate gyrus during aging have often been related to changes in microglia function (Sierra et al., 2014; de Miranda et al., 2017). It has been postulated that gene expression, activation state, and also signaling pathways involving *Cx3cr1* and *Csf1r* could be impaired during aging (Bachstetter et al., 2011; Sierra et al., 2014; de Miranda et al., 2017). By contrast, our results showed that expression of microglia markers as well as *Cx3cr1* and *Csf1r* was not changed upon aging and that activation genes were expressed at equally low levels as in the young microglia

(Figure 7D). Our results suggest that aging in the hippocampal niche could affect the abundance of the different cell populations rather than their molecular profiles, although, in order to obtain more insights about the effects of aging on gene expression, more cells need to be sequenced in the future.

DISCUSSION

Although many aspects of adult neurogenesis have been elucidated, currently little is known about the intrinsic molecular cascades that regulate NSC and progenitor behavior and about which and how niche cells contribute to this process. Rather than

taking a NSC-centric approach, we aimed to describe the cellular and molecular identities of all players involved in the process. We believe that this represents a key first step in understanding how adult neurogenesis is orchestrated.

Here we sorted every cell that does not stain for definitive neuronal markers, and we described the different cell types by *a posteriori* bioinformatics analyses. This approach has two main advantages. First, single-cell sequencing studies in a variety of tissues have demonstrated that many cell populations are heterogeneous. Therefore, unbiased sorting approaches are more likely to capture the complete cell heterogeneity as compared to known cell marker-based sorting. Second, our overall comparison of all cells present in the dentate gyrus allowed the identification of highly specific gene signatures not shared among different cell types. We believe that our study represents a powerful resource for achieving unambiguous cell identification in the neurogenic niche.

Our comprehensive dataset of 1,408 cells allowed in-depth analyses for all the cell populations identified. Our pseudo-temporal analyses of the neurogenic lineage showed that NSCs are highly heterogeneous, such that discrete subpopulations cannot be identified. They rather represent a continuum of cells that progressively downregulates genes shared with astrocytes and that are involved in quiescence maintenance while they upregulate activation genes. In agreement with the previous analyses of the pseudo-temporal gene expression cascade of SGZ NSCs (Shin et al., 2015), we did not find cells co-expressing NSCs and high levels of cell cycle markers, which were detected at high levels when cells already started expressing progenitor markers. The fact that NSCs, alike neural progenitors, do not represent a population undergoing continuous rounds of division, but only occasionally divide, could result in an overall lower expression of cell cycle markers. In addition, NSCs mostly divide to generate progenitors or quiescent NSCs (Bonaguidi et al., 2011), and the time window to identify NSCs co-expressing cell cycle markers could be very short and only right before division. Interestingly, in the SVZ, a number of NSCs expressing cell cycle markers have been found (Llorens-Bobadilla et al., 2015; Dulken et al., 2017). However, differently than in the SGZ, cells expressing NSC and progenitor markers have been identified. This could reflect distinctive features of NSCs in the two niches.

Our isolation protocol, contrary to the use of Nestin as a marker for cell isolation, yielded a large number of neuronal progenitors (see Figures S4 and S5). This allowed us to realize that NSCs are distinct from the progenitor population, and the latter, while preserving a certain degree of heterogeneity, can be categorized in more discrete subpopulations, with unique gene signatures. Many transcription factors have been found enriched in the progenitor subtypes. For some of those, critical roles have been described in brain development, but not in the context of the adult neurogenesis. For instance, *Lhx2* is important for patterning and fate specification during corticogenesis (Mangale et al., 2008; Zembrzycki et al., 2015), and *Pbx1* regulates cortical patterning (Golonzhka et al., 2015) and controls specification and survival of midbrain dopaminergic neurons (Villaescusa et al., 2016).

Astrocytes constituted a small proportion of cells in our NSC clusters, both isolated based on Nestin positivity or no-marker

expression sorting, and, in agreement with previous studies (Dulken et al., 2017; Shin et al., 2015), they could not be clustered separately from NSCs. Given the small number of isolated astrocytes, we cannot exclude that our sorting approach has a certain bias against the isolation of this population and may inspire further studies to characterize and analyze the nature of these cells.

Although NSCs *in vivo* seem not to generate oligodendrocytes, gene expression manipulation has led to NSC reprogramming to produce oligodendrocytes (Sun et al., 2015). Importantly, reprogramming of NSCs into oligodendrocytes enhances remyelination of the hippocampus after injury (Braun et al., 2015). Considering that the hippocampus is affected in demyelinating diseases (Geurts et al., 2007; Meier et al., 2004), our study, by providing cellular and molecular descriptions of oligodendrocyte stages and differentiation gene expression cascades, may aid cell reprogramming and remyelination attempts.

Finally, our study provides the single-cell molecular profiling of the dentate gyrus microglia, and it presents a comparison with Cd45^{high} cells. This could aid in the future isolation of pure populations to study the roles that different immune cells play in the hippocampus. Our results suggest that the dentate gyrus microglia are unchallenged and rather express alternative activation genes. This finding corroborates the important function of the microglia in clearing cell debris and promoting adult neurogenesis (Sierra et al., 2010). Moreover, our data suggested that, during aging, the relative proportion of microglia seems to increase, but their molecular profile remains unchanged, with implications regarding the role of microglia in age-related cognitive impairments (Koellhoffer et al., 2017).

Finally, we showed that our approach allowed us to probe cellular composition of the niche and molecular features in different conditions, for instance, in aging, as compared to homeostasis. In the future, it will be of interest to compare our data with similar single-cell transcriptome analyses under pathological conditions.

To conclude, we believe that the information provided in this paper, combined with that of single-cell RNA sequencing studies of mature and immature granule neurons in the hippocampus (Lacar et al., 2016; Zeisel et al., 2015), presents a global transcriptomic picture of the dentate gyrus.

EXPERIMENTAL PROCEDURES

Further details and an outline of resources used in this work can be found in the [Supplemental Experimental Procedures](#).

All animal experiments were approved by the local institutional review board and were performed according to local legislation. Male and female wild-type C57BL/6 mice of an age between 6 and 10 weeks or >1 year old and NestinGFP (Mignone et al., 2004) were used.

DATA AND SOFTWARE AVAILABILITY

The accession number for the data reported in this paper (provided in [Tables S4 and S5](#)) is GEO: GSE106447.

SUPPLEMENTAL INFORMATION

Supplemental Information includes Supplemental Experimental Procedures, six figures, and five tables and can be found with this article online at <https://doi.org/10.1016/j.celrep.2017.11.050>.

ACKNOWLEDGMENTS

We thank Drs. I. Heo, K. Kretschmar, T. Dayton, and O. Kopper for discussion and critical reading of the manuscript and S. van der Elst, R. van der Linden, and J. Vivie for FACS and sequencing. We also thank K.J.G. Kenswill for sharing the Nestin^{GFP} mice. B.A. was supported by a FEBS long-term fellowship and is the recipient of a Veni fellowship (NWO/VENI 863.15.015).

AUTHOR CONTRIBUTIONS

B.A. designed the study, performed the experiments with the help of A.L., analyzed the data with the help of M.M., and wrote the manuscript. J.H.v.E. performed and supervised animal experiments. A.v.O. supervised single-cell sequencing experiments. H.C. supervised the project and wrote the manuscript.

DECLARATION OF INTERESTS

The authors declare no competing interests.

Received: June 10, 2017

Revised: October 9, 2017

Accepted: November 14, 2017

Published: December 12, 2017

REFERENCES

Abiega, O., Beccari, S., Diaz-Aparicio, I., Nadjar, A., Layé, S., Leyrolle, Q., Gómez-Nicola, D., Domercq, M., Pérez-Samartín, A., Sánchez-Zafra, V., et al. (2016). Neuronal Hyperactivity Disturbs ATP Microgradients, Impairs Microglial Motility, and Reduces Phagocytic Receptor Expression Triggering Apoptosis/Microglial Phagocytosis Uncoupling. *PLoS Biol.* **14**, e1002466.

Artegiani, B., and Calegari, F. (2012). Age-related cognitive decline: can neural stem cells help us? *Aging (Albany NY)* **4**, 176–186.

Bachstetter, A.D., Morganti, J.M., Jernberg, J., Schlunk, A., Mitchell, S.H., Brewster, K.W., Hudson, C.E., Cole, M.J., Harrison, J.K., Bickford, P.C., and Gemma, C. (2011). Fractalkine and CX3CR1 regulate hippocampal neurogenesis in adult and aged rats. *Neurobiol. Aging* **32**, 2030–2044.

Bjornsson, C.S., Apostolopoulou, M., Tian, Y., and Temple, S. (2015). It takes a village: constructing the neurogenic niche. *Dev. Cell* **32**, 435–446.

Bonaguidi, M.A., Wheeler, M.A., Shapiro, J.S., Stadel, R.P., Sun, G.J., Ming, G.L., and Song, H. (2011). In vivo clonal analysis reveals self-renewing and multipotent adult neural stem cell characteristics. *Cell* **145**, 1142–1155.

Braun, S.M., Pilz, G.A., Machado, R.A., Moss, J., Becher, B., Toni, N., and Jessberger, S. (2015). Programming Hippocampal Neural Stem/Progenitor Cells into Oligodendrocytes Enhances Remyelination in the Adult Brain after Injury. *Cell Rep.* **11**, 1679–1685.

Brill, M.S., Snayyan, M., Wohlfarth, H., Ninkovic, J., Jawerka, M., Mastick, G.S., Ashery-Padan, R., Saghatelian, A., Berninger, B., and Götz, M. (2008). A *dlx2*- and *pax6*-dependent transcriptional code for periglomerular neuron specification in the adult olfactory bulb. *J. Neurosci.* **28**, 6439–6452.

Butovsky, O., Jedrychowski, M.P., Moore, C.S., Cialic, R., Lanser, A.J., Gabriely, G., Koeglperger, T., Dake, B., Wu, P.M., Doykan, C.E., et al. (2014). Identification of a unique TGF- β -dependent molecular and functional signature in microglia. *Nat. Neurosci.* **17**, 131–143.

Cherry, J.D., Olschowka, J.A., and O'Banion, M.K. (2014). Neuroinflammation and M2 microglia: the good, the bad, and the inflamed. *J. Neuroinflammation* **11**, 98.

Chhor, V., Le Charpentier, T., Lebon, S., Oré, M.V., Celador, I.L., Jossierand, J., Degos, V., Jacotot, E., Hagberg, H., Sävman, K., et al. (2013). Characterization of phenotype markers and neurotoxic potential of polarised primary microglia in vitro. *Brain Behav. Immun.* **32**, 70–85.

Colton, C.A. (2009). Heterogeneity of microglial activation in the innate immune response in the brain. *J. Neuroimmune Pharmacol.* **4**, 399–418.

de Miranda, A.S., Zhang, C.J., Katsumoto, A., and Teixeira, A.L. (2017). Hippocampal adult neurogenesis: Does the immune system matter? *J. Neurol. Sci.* **372**, 482–495.

Dulken, B.W., Leeman, D.S., Boutet, S.C., Hebestreit, K., and Brunet, A. (2017). Single-Cell Transcriptomic Analysis Defines Heterogeneity and Transcriptional Dynamics in the Adult Neural Stem Cell Lineage. *Cell Rep.* **18**, 777–790.

Gautier, E.L., Shay, T., Miller, J., Greter, M., Jakubczak, C., Ivanov, S., Helft, J., Chow, A., Elpek, K.G., Gordonov, S., et al.; Immunological Genome Consortium (2012). Gene-expression profiles and transcriptional regulatory pathways that underlie the identity and diversity of mouse tissue macrophages. *Nat. Immunol.* **13**, 1118–1128.

Geurts, J.J., Bö, L., Roosendaal, S.D., Hazes, T., Daniëls, R., Barkhof, F., Witter, M.P., Huitinga, I., and van der Valk, P. (2007). Extensive hippocampal demyelination in multiple sclerosis. *J. Neuropathol. Exp. Neurol.* **66**, 819–827.

Golonzhka, O., Nord, A., Tang, P.L., Lindtner, S., Ypsilanti, A.R., Ferretti, E., Visel, A., Selleri, L., and Rubenstein, J.L. (2015). *Pbx* Regulates Patterning of the Cerebral Cortex in Progenitors and Postmitotic Neurons. *Neuron* **88**, 1192–1207.

Gomez Perdiguer, E., Schulz, C., and Geissmann, F. (2013). Development and homeostasis of “resident” myeloid cells: the case of the microglia. *Glia* **61**, 112–120.

Gonçalves, J.T., Schafer, S.T., and Gage, F.H. (2016). Adult Neurogenesis in the Hippocampus: From Stem Cells to Behavior. *Cell* **167**, 897–914.

Grün, D., and van Oudenaarden, A. (2015). Design and Analysis of Single-Cell Sequencing Experiments. *Cell* **163**, 799–810.

Grün, D., Muraro, M.J., Boisset, J.C., Wiebrands, K., Lyubimova, A., Dharmadhikari, G., van den Born, M., van Es, J., Jansen, E., Clevers, H., et al. (2016). De Novo Prediction of Stem Cell Identity using Single-Cell Transcriptome Data. *Cell Stem Cell* **19**, 266–277.

Hagihara, H., Ohira, K., Toyama, K., and Miyakawa, T. (2011). Expression of the AMPA Receptor Subunits GluR1 and GluR2 is Associated with Granule Cell Maturation in the Dentate Gyrus. *Front. Neurosci.* **5**, 100.

Hickman, S.E., Kingery, N.D., Ohsumi, T.K., Borowsky, M.L., Wang, L.C., Means, T.K., and El Khoury, J. (2013). The microglial sensome revealed by direct RNA sequencing. *Nat. Neurosci.* **16**, 1896–1905.

Hodge, R.D., Garcia, A.J., 3rd, Elsen, G.E., Nelson, B.R., Mussar, K.E., Reiner, S.L., Ramirez, J.M., and Hevner, R.F. (2013). *Tbr2* expression in Cajal-Retzius cells and intermediate neuronal progenitors is required for morphogenesis of the dentate gyrus. *J. Neurosci.* **33**, 4165–4180.

Kang, W., and Hébert, J.M. (2015). FGF Signaling Is Necessary for Neurogenesis in Young Mice and Sufficient to Reverse Its Decline in Old Mice. *J. Neurosci.* **35**, 10217–10223.

Kempermann, G., Song, H., and Gage, F.H. (2015). Neurogenesis in the Adult Hippocampus. *Cold Spring Harb. Perspect. Biol.* **7**, a018812.

Knobloch, M., Braun, S.M., Zurkirchen, L., von Schoultz, C., Zamboni, N., Araújo-Bravo, M.J., Kovacs, W.J., Karalay, O., Suter, U., Machado, R.A., et al. (2013). Metabolic control of adult neural stem cell activity by Fasn-dependent lipogenesis. *Nature* **493**, 226–230.

Koellhoffer, E.C., McCullough, L.D., and Ritzel, R.M. (2017). Old Maids: Aging and Its Impact on Microglia Function. *Int. J. Mol. Sci.* **18**, E769.

Kriegstein, A., and Alvarez-Buylla, A. (2009). The glial nature of embryonic and adult neural stem cells. *Annu. Rev. Neurosci.* **32**, 149–184.

La Manno, G., Gyllborg, D., Codeluppi, S., Nishimura, K., Salto, C., Zeisel, A., Borm, L.E., Stott, S.R., Toledo, E.M., Villaescusa, J.C., et al. (2016). Molecular Diversity of Midbrain Development in Mouse, Human, and Stem Cells. *Cell* **167**, 566–580.e19.

Lacar, B., Linker, S.B., Jaeger, B.N., Krishnaswami, S., Barron, J., Kelder, M., Parylak, S., Paquola, A., Venepally, P., Novotny, M., et al. (2016). Nuclear RNA-seq of single neurons reveals molecular signatures of activation. *Nat. Commun.* **7**, 11022.

Lake, B.B., Ai, R., Kaeser, G.E., Salathia, N.S., Yung, Y.C., Liu, R., Wildberg, A., Gao, D., Fung, H.L., Chen, S., et al. (2016). Neuronal subtypes and diversity

- p revealed by single-nucleus RNA sequencing of the human brain.
- Science*
- 352, 1586–1590.
- Liu, S.J., Nowakowski, T.J., Pollen, A.A., Lui, J.H., Horlbeck, M.A., Attenello, F.J., He, D., Weissman, J.S., Kriegstein, A.R., Diaz, A.A., and Lim, D.A. (2016). Single-cell analysis of long non-coding RNAs in the developing human neocortex. *Genome Biol.* 17, 67.
- Llorens-Bobadilla, E., Zhao, S., Baser, A., Saiz-Castro, G., Zwadlo, K., and Martin-Villalba, A. (2015). Single-Cell Transcriptomics Reveals a Population of Dormant Neural Stem Cells that Become Activated upon Brain Injury. *Cell Stem Cell* 17, 329–340.
- Luo, Y., Coskun, V., Liang, A., Yu, J., Cheng, L., Ge, W., Shi, Z., Zhang, K., Li, C., Cui, Y., et al. (2015). Single-cell transcriptome analyses reveal signals to activate dormant neural stem cells. *Cell* 161, 1175–1186.
- Mangale, V.S., Hirokawa, K.E., Satyaki, P.R., Gokulchandran, N., Chikbire, S., Subramanian, L., Shetty, A.S., Martynoga, B., Paul, J., Mai, M.V., et al. (2008). Lhx2 selector activity specifies cortical identity and suppresses hippocampal organizer fate. *Science* 319, 304–309.
- Marques, S., Zeisel, A., Codeluppi, S., van Bruggen, D., Mendanha Falcão, A., Xiao, L., Li, H., Häring, M., Hochgerner, H., Romanov, R.A., et al. (2016). Oligodendrocyte heterogeneity in the mouse juvenile and adult central nervous system. *Science* 352, 1326–1329.
- Meier, S., Bräuer, A.U., Heimrich, B., Nitsch, R., and Savaskan, N.E. (2004). Myelination in the hippocampus during development and following lesion. *Cell. Mol. Life Sci.* 67, 1082–1094.
- Mignone, J.L., Kukekov, V., Chiang, A.S., Steindler, D., and Enikolopov, G. (2004). Neural stem and progenitor cells in nestin-GFP transgenic mice. *J. Comp. Neurol.* 469, 311–324.
- Muraro, M.J., Dharmadhikari, G., Grün, D., Groen, N., Dielen, T., Jansen, E., van Gurp, L., Engelse, M.A., Carlotti, F., de Koning, E.J., and van Oudenaarden, A. (2016). A Single-Cell Transcriptome Atlas of the Human Pancreas. *Cell Syst.* 3, 385–394.e3.
- Neumann, H., and Takahashi, K. (2007). Essential role of the microglial triggering receptor expressed on myeloid cells-2 (TREM2) for central nervous tissue immune homeostasis. *J. Neuroimmunol.* 184, 92–99.
- Ninkovic, J., and Götz, M. (2013). Fate specification in the adult brain—lessons for eliciting neurogenesis from glial cells. *BioEssays* 35, 242–252.
- Ninkovic, J., Steiner-Mezzadri, A., Jawerka, M., Akinci, U., Masserdotti, G., Petricca, S., Fischer, J., von Holst, A., Beckers, J., Lie, C.D., et al. (2013). The BAF complex interacts with Pax6 in adult neural progenitors to establish a neurogenic cross-regulatory transcriptional network. *Cell Stem Cell* 13, 403–418.
- Pollen, A.A., Nowakowski, T.J., Chen, J., Retallack, H., Sandoval-Espinosa, C., Nicholas, C.R., Shuga, J., Liu, S.J., Oldham, M.C., Diaz, A., et al. (2015). Molecular identity of human outer radial glia during cortical development. *Cell* 163, 55–67.
- Prinz, M., and Priller, J. (2014). Microglia and brain macrophages in the molecular age: from origin to neuropsychiatric disease. *Nat. Rev. Neurosci.* 15, 300–312.
- Sasaki, A. (2017). Microglia and brain macrophages: An update. *Neuropathology* 37, 452–464.
- Shin, J., Berg, D.A., Zhu, Y., Shin, J.Y., Song, J., Bonaguidi, M.A., Enikolopov, G., Nauen, D.W., Christian, K.M., Ming, G.L., and Song, H. (2015). Single-Cell RNA-Seq with Waterfall Reveals Molecular Cascades underlying Adult Neurogenesis. *Cell Stem Cell* 17, 360–372.
- Sierra, A., Encinas, J.M., Deudero, J.J., Chancey, J.H., Enikolopov, G., Overstreet-Wadiche, L.S., Tsirka, S.E., and Maletic-Savatic, M. (2010). Microglia shape adult hippocampal neurogenesis through apoptosis-coupled phagocytosis. *Cell Stem Cell* 7, 483–495.
- Sierra, A., Beccari, S., Diaz-Aparicio, I., Encinas, J.M., Comeau, S., and Tremblay, M.E. (2014). Surveillance, phagocytosis, and inflammation: how never-resting microglia influence adult hippocampal neurogenesis. *Neural Plast.* 2014, 610343.
- Sun, G.J., Zhou, Y., Ito, S., Bonaguidi, M.A., Stein-O'Brien, G., Kawasaki, N.K., Modak, N., Zhu, Y., Ming, G.L., and Song, H. (2015). Latent tri-lineage potential of adult hippocampal neural stem cells revealed by Nf1 inactivation. *Nat. Neurosci.* 18, 1722–1724.
- Tasic, B., Menon, V., Nguyen, T.N., Kim, T.K., Jarsky, T., Yao, Z., Levi, B., Gray, L.T., Sorensen, S.A., Dolbeare, T., et al. (2016). Adult mouse cortical cell taxonomy revealed by single cell transcriptomics. *Nat. Neurosci.* 19, 335–346.
- Trapnell, C. (2015). Defining cell types and states with single-cell genomics. *Genome Res.* 25, 1491–1498.
- Villaescusa, J.C., Li, B., Toledo, E.M., Rivetti di Val Cervo, P., Yang, S., Stott, S.R., Kaiser, K., Islam, S., Gyllborg, D., Laguna-Goya, R., et al. (2016). A PBX1 transcriptional network controls dopaminergic neuron development and is impaired in Parkinson's disease. *EMBO J.* 35, 1963–1978.
- Walker, T.L., Wierick, A., Sykes, A.M., Waldau, B., Corbeil, D., Carmeliet, P., and Kempermann, G. (2013). Prominin-1 allows prospective isolation of neural stem cells from the adult murine hippocampus. *J. Neurosci.* 33, 3010–3024.
- Yoshida, M., Suda, Y., Matsuo, I., Miyamoto, N., Takeda, N., Kuratani, S., and Aizawa, S. (1997). Emx1 and Emx2 functions in development of dorsal telencephalon. *Development* 124, 101–111.
- Zeisel, A., Muñoz-Manchado, A.B., Codeluppi, S., Lönnerberg, P., La Manno, G., Juréus, A., Marques, S., Munguba, H., He, L., Betscholtz, C., et al. (2015). Brain structure. Cell types in the mouse cortex and hippocampus revealed by single-cell RNA-seq. *Science* 347, 1138–1142.
- Zembrzycki, A., Perez-Garcia, C.G., Wang, C.F., Chou, S.J., and O'Leary, D.D. (2015). Postmitotic regulation of sensory area patterning in the mammalian neocortex by Lhx2. *Proc. Natl. Acad. Sci. USA* 112, 6736–6741.
- Zhao, C., Deng, W., and Gage, F.H. (2008). Mechanisms and functional implications of adult neurogenesis. *Cell* 132, 645–660.